

## Statistics of static avalanches in a random pinning landscape

Pierre Le Doussal,<sup>1</sup> A. Alan Middleton,<sup>2</sup> and Kay Jörg Wiese<sup>1</sup>

<sup>1</sup>*Laboratoire de Physique Théorique de l'École Normale Supérieure, CNRS, 24 rue Lhomond, 75005 Paris, France*

<sup>2</sup>*Department of Physics, Syracuse University, Syracuse, New York 13244, USA*

(Received 21 March 2008; published 7 May 2009)

We study the minimum-energy configuration of a  $d$ -dimensional elastic interface in a random potential tied to a harmonic spring. As a function of the spring position, the center of mass of the interface changes in discrete jumps, also called shocks or “static avalanches.” We obtain analytically the distribution of avalanche sizes and its cumulants within an  $\epsilon=4-d$  expansion from a tree and one-loop resummation using functional renormalization. This is compared with exact numerical minimizations of interface energies for random-field disorder in  $d=2,3$ . Connections to dynamic avalanches are mentioned.

DOI: 10.1103/PhysRevE.79.050101

PACS number(s): 05.10.Cc, 02.60.Pn, 75.10.Nr

In numerous systems, the equilibrium or nonequilibrium response to perturbations is not smooth and involves jumps, avalanches, or bursts. In systems at the brink of instability, with many metastable states, it is often self-organized and critical with power-law tails for the probability of large events. This is observed ubiquitously in systems with heterogeneities, such as Barkhausen noise and hysteresis in magnets, field response of superconductors, contact line of fluids, cracks, granular matter, dry friction, and earthquakes. Sandpile automata [1] and elastic media pinned by quenched disorder [2] have been studied as simple models for these phenomena. Relations between sandpiles and interface depinning [3,4] and between sandpile models and loop-erased walks [5–7] have proved fruitful, especially in  $d=2$ , where conformal field theory can be used [8]. Despite much effort it has proven difficult to obtain analytical results, e.g., for the distribution of the size  $s$  of avalanches (defined below), except in mean-field models for sandpiles [9] and for random-field Ising magnets [10] as well as for a toy model for avalanches at depinning [2], which all yield  $P(s) \sim s^{-\tau}$ , with  $\tau=3/2$ . Scaling arguments for sandpiles [1,7] and for depinning [11,12] were developed together with numerical analysis [3,13,14]. The functional renormalization-group (RG) (FRG) theory for pinned systems has led to detailed predictions for, e.g., the roughness of interfaces but, until now, has failed to describe discontinuous jump processes [11,15–17]. Hence it remains an outstanding issue to find a limit where mean-field theory is valid, prove this, and develop a controlled field-theoretic expansion around it. Such results should allow for a clarification of the differences between equilibrium and nonequilibrium avalanches, which distinction has been questioned in a model for magnetic hysteresis [18].

The aim of this Rapid Communication is to provide a first analytical calculation of the distribution of avalanche sizes in a static equilibrium setting using FRG and to make comparisons with numerical calculations. It opens the way to a closely related calculation for depinning [19]. As demonstrated in our previous work [20], a model which allows a precise FRG treatment and comparison with numerics, both in statics and dynamics, consists of an elastic interface in a random potential parameterized by a (scalar) height field  $u(x)$  and submitted to an external parabolic well, i.e., a spring, centered at  $u=w$ ,

$$\mathcal{H}[u;w] = \int d^d x \frac{1}{2} [\nabla u(x)]^2 + V(x, u(x)) + \frac{m^2}{2} [u(x) - w]^2. \quad (1)$$

This model is realized in experiments, e.g., in contact-line depinning, where  $m^2$  relates to the capillary length set by gravity, or in magnetic interfaces, where  $m^2$  is proportional to an external field gradient. We are interested in energy minimization as  $w$  is varied in a given realization of the random potential  $V(x, u)$ . We denote  $\hat{V}(w) = \min_{\{u(x)\}} \mathcal{H}[u;w]$  as the optimal energy and  $u(x;w)$  as the optimal interface position. The force per unit volume exerted by the spring is  $\hat{V}'(w) = m^2[w - u(w)]$ , where  $u(w) := L^{-d} \int d^d x u(x;w)$  is the center-of-mass position and  $L^d$  is the volume of the system. We study the three main universality classes by choosing the disorder correlator  $\overline{V(x, u)V(x', 0)}$  either short range in  $u$  [random bond (RB) class], periodic in  $u$  [random periodic (RP) class], or long range, i.e.,  $[V(x, u) - V(x', 0)]^2 \sim |u|$  (the random-field (RF) class [11,15–17,20,21]).

Although we often use the language of dynamics, one should emphasize the difference between the static problem studied here, where the interface finds the global energy minimum for each  $w$ , and the dynamic one, where  $w(t)$  grows very slowly, and the interface visits a deterministic sequence of metastable states.[22] In the scaling limit  $m \rightarrow 0$ , on which we focus here, the first case is about interface configurations of zero-temperature equilibrium [20], whereas the latter one is about critical depinning [23,24]. Despite these differences, depinning and statics are close cousins, and some differences within the FRG are found only beyond one loop [17].

As shown previously [15,20,21,25,26], the optimal interface is statistically self-affine with  $[u(x) - u(0)]^2 \sim |x|^{2\zeta}$ , where the roughness exponent  $\zeta$  depends on the class of disorder and has a known  $\epsilon=4-d$  expansion [17]:  $\zeta = \epsilon/3$  for RF,  $\zeta=0$  for RP, and  $\zeta=0.2083\epsilon+0.00686\epsilon^2$  for RB (and  $\zeta=2/3$  in  $d=1$ ). This holds for scales  $L_c < L < L_m$ , where  $L_c$  is the Larkin length (here of the order of the microscopic cutoff) and  $L_m \sim 1/m$  is the large scale cutoff induced by the harmonic well. It is useful to picture the interface as a collection of  $(L/L_m)^d$  regions pinned almost independently.

We confirm that  $u(x;w)$  is an increasing function of  $w$  which can be decomposed into smooth parts, negligible in the scaling limit  $m \rightarrow 0$ , and jumps (alias “shocks” or static avalanches) occurring at position  $w_i$  as

$$u(x;w) = \sum_i S_i^x \theta(w - w_i), \quad S_i := \int d^d x S_i^x, \quad (2)$$

where  $S_i^x$  is the size of the shock or avalanche labeled  $i$  at position  $x$  and  $\theta(w)$  is the step function. The avalanche-size distribution defined from an average over samples,

$$\sum_i \overline{\delta(S - S_i) \delta(w - w_i)} = \rho(S) = \rho_0 P(S), \quad (3)$$

can equivalently be defined from a translational average in a given sample. Here  $P(S)$  is the normalized size distribution and  $\rho_0 dw$  is the average number of shocks in an interval  $dw$ . The scaling ansatz,

$$\rho(S) = L^d m^\rho S^{-\tau} \tilde{\rho}(Sm^{d+\xi}), \quad (4)$$

is shown below to hold within the  $\epsilon$  expansion and verified by our numerics. The center of mass follows on average the spring, i.e.,  $u(w) - w$  is bounded, thus  $u'(w) = 1$ . This allows us to relate the shock rate and the first moment  $L^{-d} \rho_0 \langle S \rangle = 1$ , where  $\langle S^n \rangle := \int dS S^n P(S)$  denotes the normalized moments. It implies for  $\tau < 2$  the exponent relation  $\rho = (2 - \tau)(d + \xi)$ . The distribution is qualitatively different for (i)  $\tau < 1$  when a unique scale  $S_m \sim m^{-(d+\xi)}$  exists, i.e.,  $P(S) = S_m^{-1} \tilde{P}(S/S_m)$ , and (ii)  $1 < \tau < 2$ , where

$$P(S) = C S_0^{-1} (S/S_0)^{-\tau} f(S/S_m), \quad (5)$$

and typical avalanches are of the order of the microscopic (UV) cutoff  $S_0$ , while moments  $\langle S^p \rangle$  with  $p > \tau - 1$  are controlled by rare avalanches of size  $\sim S_m$ , the large-scale cutoff. As seen from Eq. (2), the function  $u(w) - w$  exhibits jumps  $S_i$  at position  $w_i$ , thus  $[u(w) - w]^n$  has jumps of size  $S_i^n$ . More precisely, the  $n$ th Kolmogorov cumulant [27,28] is (for  $w > 0$ )

$$K^{(n)}(w) := m^{2n} L^{(n-1)d} \overline{[u(w) - w - u(0)]^n}^c = \frac{\langle S^n \rangle}{\langle S \rangle} w + O(w^2), \quad (6)$$

understood as the probability  $\sim w$  that there is a shock, times its magnitude  $S_i^n$ , normalized due to the constraint  $u'(w) = 1$ . For  $n=2$ ,  $K^{(2)}$  relates to the renormalized disorder correlator  $\Delta(w)$ , computed to  $O(\epsilon^2)$  in Ref. [17]. It is famous for developing a cusp, here nicely interpreted in terms of the second moment of avalanche sizes, i.e.,  $-2\Delta'(0^+) = m^4 \langle S^2 \rangle / \langle S \rangle$ . We now compute the avalanche-size distribution using the generating function

$$L^{-d} (\overline{e^{\lambda L^d [u(w) - w - u(0)]}} - 1) = Z(\lambda) w + O(w^2),$$

$$Z(\lambda) = \frac{1}{\langle S \rangle} (\langle e^{\lambda S} \rangle - 1 - \lambda \langle S \rangle), \quad (7)$$

for  $w > 0$ . We have computed the leading nonanalyticity of Eq. (7) from (i) a Legendre transform of the replicated effec-

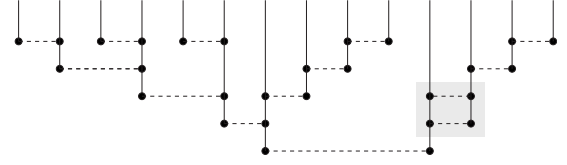
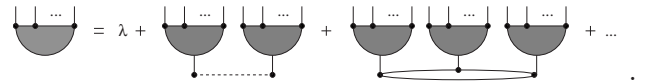


FIG. 1. In mean field, diagrams generated by Eq. (8) at  $\alpha=0$  (one example shown here) have a tree structure, up to simple one-loop corrections to disorder, i.e.,  $\Delta'(0^+)$  (shaded in gray). As in [17], the solid lines are propagators and the dashed lines are disorder correlators. Intuitively, solid lines represent successive local events (e.g., spin flips) in the avalanche and the dashed lines represent correlations between them due to disorder.

tive action  $\Gamma$  computed order by order in  $\epsilon$  and (ii) a direct perturbative expansion without using replicas. The calculation is more involved than usually for the FRG: the size distribution already at order  $O(\epsilon^0)$  requires a summation of all tree diagrams. The latter could be termed mean field but with the proviso that the scale of  $S$  involves  $\Delta'(0^+)$  computed to  $O(\epsilon)$ . Here we compute to order  $O(\epsilon)$ , which amounts to summing all trees and single loops; for details see [29]. The main result is that  $Z(\lambda)$  satisfies a remarkable self-consistent equation to one loop order,

$$\tilde{Z}(\lambda) = \lambda + \tilde{Z}(\lambda)^2 + \alpha \sum_{n \geq 3} (n+1) 2^{n-2} i_n \tilde{Z}(\lambda)^n, \quad (8)$$

where  $Z(\lambda) = \frac{m^4}{|\Delta'(0^+)|} \tilde{Z}(\lambda m^{-4} |\Delta'(0^+)|) - \lambda$ ,  $i_n = \tilde{I}_n / (\epsilon \tilde{I}_2)$ ,  $\tilde{I}_n = \int_k (k^2 + 1)^{-n}$ , and  $\alpha = -\epsilon \tilde{I}_2 m^{-\epsilon} \Delta''(0^+)$ . It can graphically be written as



The type of resummed diagrams is presented in Fig. 1. Since  $\alpha = O(\epsilon)$ , to leading order one solves Eq. (8) setting  $\alpha = 0$ . This yields  $\tilde{Z}_{\text{MF}}(\lambda) = \frac{1}{2}(1 - \sqrt{1 - 4\lambda})$ , identical to the generating function of the number of rooted binary planar trees with  $n$  leaves [30], and a size distribution, with  $\tau = 3/2$ ,

$$P_{\text{MF}}(S) = \frac{\langle S \rangle}{2\sqrt{\pi}} S_m^{-1/2} S^{-3/2} e^{-S/(4S_m)}. \quad (9)$$

This is valid for  $S \gg S_0$ , such that the moments with  $p > \frac{1}{2}$  are independent of the nonuniversal small-scale cutoff  $S_0$ . Hence the rigorous summation of tree diagrams in the FRG yields the same  $P_{\text{MF}}(S)$  as that of a mean-field toy model for dynamic avalanches [2] and that of mean-field sandpiles [9]. In addition, since the FRG is a first-principles method, it predicts  $S_m = cm^{-d-\xi}$ , where  $c = (\epsilon \tilde{I}_2) |\tilde{\Delta}'(0^+)|$  is obtained from the FRG fixed point for the rescaled correlator  $\tilde{\Delta}(u) = (\epsilon \tilde{I}_2) m^{-\epsilon+2\xi} \Delta(um^{-\xi})$  and depends on the universality class [29]. Since  $\tau > 1$  the scale  $\langle S \rangle \sim S_0^{-1} S_m^{2-\tau}$  remains undetermined and UV cut-off dependent. Equation (8), seen as a convolution equation for  $P(S)$ , may allow one to put the physical picture in [2] on a more rigorous footing.

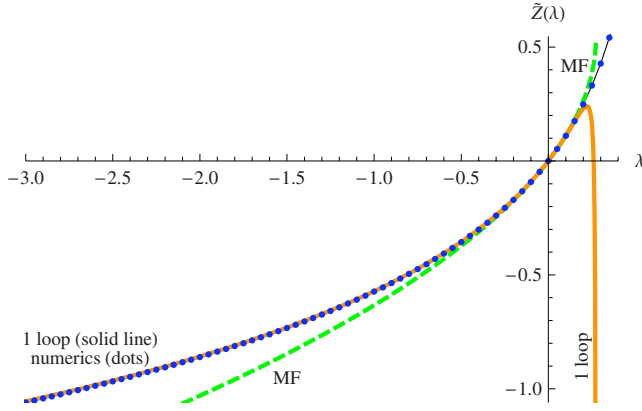


FIG. 2. (Color online)  $\tilde{Z}(\lambda)$  for RF,  $d=2$ . The MF and one-loop analytical curves are given in the text and  $\lambda$  being rescaled to reproduce the numerically measured second moment. While the MF result differs substantially from the numerical measurement, the one-loop curve, i.e., Eq. (11) with  $\alpha$  given by Eq. (10) setting  $\epsilon=2$  and  $\zeta_1=1/3$ , coincides for all negative  $\lambda$ , and almost up to the singularity for  $\lambda>0$ . Changing  $\epsilon$  from 2 to 2.1 or 1.9 already results in a visible disagreement for  $\lambda<0$ .

To next order in  $\epsilon$  we solve Eq. (8), which includes higher branchings with a universal dimensionless rate

$$\alpha = -\frac{1}{3}(1 - \zeta_1)\epsilon \quad (10)$$

at the fixed point, where  $\zeta = \zeta_1\epsilon + O(\epsilon^2)$  and  $i_n = 1/2(n-1)(n-2)$  in  $d=4$ . It yields

$$\begin{aligned} \tilde{Z}(\lambda) = & \frac{1}{2}[1 - \sqrt{1-4\lambda}] + \frac{\alpha}{4\sqrt{1-4\lambda}}[\log(1-4\lambda) \\ & \times (3\lambda + \sqrt{1-4\lambda} - 1) - 2(2\lambda + \sqrt{1-4\lambda} - 1)] + O(\alpha^2), \end{aligned} \quad (11)$$

from which one can calculate the universal ratios,

$$\begin{aligned} r_n := & \langle S^{n+1} \rangle \langle S^{n-1} \rangle \langle S^n \rangle^{-2} \\ = & \frac{2n-1}{2n-3} - \frac{\epsilon}{3}(1-\zeta_1) \frac{n\Gamma\left(n-\frac{3}{2}\right) + \sqrt{\pi}\Gamma(n-1)}{(2n-3)^2\Gamma\left(n-\frac{3}{2}\right)} + O(\epsilon^2), \end{aligned} \quad (12)$$

for any real  $n > 3/2$ , with  $\zeta_1=1/3$  for RF,  $\zeta_1=0$  for RP, and

TABLE I. Universal amplitude ratios with statistical and systematic errors (in this order) for numerics; there is a systematic error since the measured ratios decrease with decreasing mass. For  $d=2$ , the decrease which we take as systematic error was measured from masses  $m^2=0.025$ ,  $m^2=0.00125$ , and  $m^2=0.000625$  (whose values are given). For  $d=3$ , the corresponding one is measured for the two smallest masses  $m^2=0.0025$  and  $m^2=0.00125$  (with values from the latter).

RF	$r_2$	$r_3$	$r_4$
Mean field	3	1.67	1.4
$d=3$ , Eq. (12)	2.33	1.54	1.34
$d=3$ , numerics	$2.25 \pm 0.05 \pm 0.2$	$1.48 \pm 0.04 \pm 0.14$	$1.27 \pm 0.02 \pm 0.13$
$d=2$ , Eq. (12)	1.66	1.42	1.28
$d=2$ , numerics	$1.95 \pm 0.02 \pm 0.06$	$1.38 \pm 0.02 \pm 0.06$	$1.21 \pm 0.02 \pm 0.06$

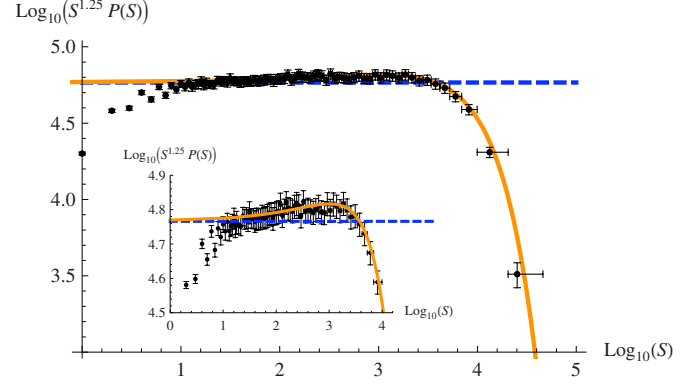


FIG. 3. (Color online) Numerically computed normalized avalanche distribution  $P(S)$ , for random-field disorder and  $d=2$  ( $\zeta=2/3$ ), multiplied by  $S^\tau$  with  $\tau=1.25$  [from Eq. (16)] to emphasize deviations from the power law  $P(S) \sim S^{-1.25}$ . Error bars are  $3\sigma$  errors for  $P(S)$  and the size of the box for  $S$ . The solid curve is a one-parameter fit to Eq. (13), with  $\mathcal{S}_m=3500$ ,  $\tau=1.25$ ,  $\alpha$  given by Eq. (10) with  $\zeta_1=1/3$ ,  $\epsilon=2$ , and the corresponding values for  $B, C$  given in the text. We use the measured value for  $\langle S \rangle$  in Eq. (13) hence there is no additional free parameter. The dashed line is a constant (guide to the eyes). Inset: blowup of main plot. The best fit to a pure power law would give  $\tau=1.23$  and to a power law times exponential  $\tau=1.2$ .

$\zeta_1=0.283$  for RB. Upon inversion of the Laplace transform one finds

$$P(S) = \frac{\langle S \rangle}{2\sqrt{\pi}} \mathcal{S}_m^{\tau-2} A S^{-\tau} \exp\left(C \sqrt{\frac{S}{\mathcal{S}_m}} - \frac{B}{4} \left[\frac{S}{\mathcal{S}_m}\right]^\delta\right) \quad (13)$$

for  $S \gg \mathcal{S}_0$ , with  $C = -\frac{1}{2}\sqrt{\pi}\alpha$ ,  $B = 1 - \alpha(1 + \frac{\gamma_E}{4})$ ,  $A = 1 + \frac{1}{8}(2 - 3\gamma_E)\alpha$ ,  $\gamma_E = 0.577216$ , and exponents

$$\tau = \frac{3}{2} + \frac{3}{8}\alpha = \frac{3}{2} - \frac{1}{8}(1 - \zeta_1)\epsilon + O(\epsilon^2), \quad (14)$$

$$\delta = 1 - \frac{\alpha}{4} = 1 + \frac{1}{12}(1 - \zeta_1)\epsilon. \quad (15)$$

Note that the decay of large avalanches becomes stretched (sub)exponential (in  $d=0$  for RF,  $\delta=3$ ). We note that our result for  $\tau$  agrees to  $O(\epsilon)$  with the conjecture

$$\tau = 2 - \frac{2}{d + \zeta}, \quad (16)$$

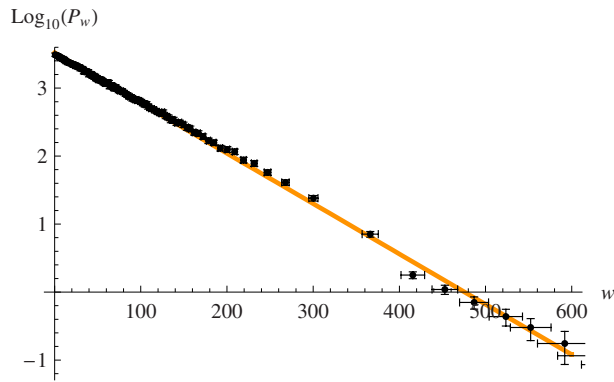


FIG. 4. (Color online) Distribution of intervals between jumps, in units of the step-size  $\delta w=0.002$ . Error bars are  $3\sigma$  errors.

equivalent to  $\rho=2$ . It was presented for *depinning* [11,12] and for the  $\tau_s=4/3$  exponent of the number of topplings in a sandpile model in  $d=3$  [7], which may be compared to the RP class. Since assumptions leading to Eq. (16) are not rigorous, our first-principles calculation confirms this to one loop and leaves open the possibility of higher-loop corrections. Our results are straightforwardly extended to the case of nonlocal elasticity [29] and dynamics [19].

Exact numerical calculation of minimum-energy interfaces has been performed for a RF Ising model using the very efficient (polynomial) max-flow algorithms, as in [20]. We first measured the generating function  $\tilde{Z}(\lambda)$  displayed on Fig. 2 for RF disorder in three dimensions ( $d=2$ ). It is easier to measure numerically than the avalanche-size distribution

since it does not require binning. We see that the  $O(\epsilon)$  result is in excellent agreement with the numerics up to  $\lambda \approx \frac{1}{2}$ . The (corrected) avalanche distribution is presented on Fig. 3. We measure (also see Table I) for values of the universal amplitude ratios

$$\tau = 1.25 \pm 0.02(\text{RF}, d=2), \quad \tau = 1.37 \pm 0.03(\text{RF}, d=3). \quad (17)$$

This is compatible with Eq. (16). Note that the extra stretched-exponential term  $C$  in Eq. (13) (which could not be interpreted as summation of a pre-exponential power) leads to a bump which can clearly be seen in the numerics on Fig. 3. Finally we have measured (see Fig. 4) the distribution of the intervals between successive jumps (occurring at positions  $w=w^i$ ) and found it to be very close to a pure exponential.

To conclude, using functional RG we have performed an expansion around the upper critical dimension to obtain the avalanche or shock distribution in the statics. It compares well with the numerics. Preliminary results [19] indicate that the above mean-field and one-loop results also hold for depinning (with the corresponding values for  $\zeta$ ); two-loop calculations are in progress to further check conjecture (16) and quantify the difference between static and dynamic avalanches.

We acknowledge very useful discussions with Karin Dahmen and Andrei Fedorenko and support from NSF under Grant No. 0606424 (A.A.M.) and ANR under Program No. 05-BLAN-0099-01 (P.L.D. and K.W.).

- 
- [1] P. Bak *et al.*, Phys. Rev. Lett. **59**, 381 (1987); D. Dhar, Physica A **369**, 29 (2006); Physica A **263**, 4 (1999); E. V. Ivashkevich and V. B. Priezzhev, Physica A **254**, 97 (1998).  
[2] D. S. Fisher, Phys. Rep. **301**, 113 (1998).  
[3] O. Narayan and A. A. Middleton, Phys. Rev. B **49**, 244 (1994).  
[4] M. Alava, J. Phys.: Condens. Matter **14**, 2353 (2002); M. Alava and M. A. Munoz, Phys. Rev. E **65**, 026145 (2002).  
[5] S. N. Majumdar and D. Dhar, Physica A **185**, 129 (1992).  
[6] V. B. Priezzhev, J. Stat. Phys. **98**, 667 (2000).  
[7] H. Agrawal and D. Dhar, Phys. Rev. E **63**, 056115 (2001).  
[8] V. S. Poghosyan *et al.*, Phys. Lett. B **659**, 768 (2008).  
[9] C. Tang and P. Bak, J. Stat. Phys. **51**, 797 (1988); M. Stapleton and K. Christensen, e-print arXiv:cond-mat/0510626; D. Dhar and S. N. Majumdar, J. Phys A **23**, 4333 (1990).  
[10] K. Dahmen and J. P. Sethna, Phys. Rev. B **53**, 14872 (1996).  
[11] O. Narayan and D. S. Fisher, Phys. Rev. B **48**, 7030 (1993).  
[12] S. Zapperi *et al.*, Phys. Rev. B **58**, 6353 (1998).  
[13] A. A. Middleton and D. S. Fisher, Phys. Rev. B **47**, 3530 (1993).  
[14] S. Lübeck and K. D. Usadel, Phys. Rev. E **56**, 5138 (1997).  
[15] D. S. Fisher, Phys. Rev. Lett. **56**, 1964 (1986); Phys. Rev. B **31**, 7233 (1985).  
[16] T. Nattermann *et al.*, J. Phys. II **2**, 1483 (1992).  
[17] P. Chauve *et al.*, Phys. Rev. Lett. **86**, 1785 (2001); P. Le Doussal *et al.*, Phys. Rev. E **69**, 026112 (2004); Phys. Rev. B **66**, 174201 (2002).  
[18] Y. Liu and K. A. Dahmen, e-print arXiv:cond-mat/0609609.  
[19] A. Fedorenko, P. Le Doussal, and K. J. Wiese (unpublished).  
[20] A. A. Middleton *et al.*, Phys. Rev. Lett. **98**, 155701 (2007).  
[21] G. Blatter *et al.* Rev. Mod. Phys. **66**, 1125 (1994); T. Giamarchi and P. Le Doussal, Phys. Rev. B **52**, 1242 (1995); T. Nattermann and S. Scheidl, Adv. Phys. **49**, 607 (2000).  
[22] A. A. Middleton, Phys. Rev. Lett. **68**, 670 (1992).  
[23] P. Le Doussal and K. J. Wiese, EPL **77**, 66001 (2007).  
[24] A. Rosso *et al.*, Phys. Rev. B **75**, 220201(R) (2007).  
[25] A. A. Middleton, Phys. Rev. E **52**, R3337 (1995); D. McNamara *et al.*, Phys. Rev. B **60**, 10062 (1999).  
[26] J. D. Noh and H. Rieger, Phys. Rev. Lett. **87**, 176102 (2001).  
[27] P. Le Doussal, Europhys. Lett. **76**, 457 (2006); e-print arXiv:cond-mat/0605490; e-print arXiv:0809.1192.  
[28] Shocks for manifolds are a generalization [27] of shocks in decaying Burgers turbulence, and linearity of  $K^{(3)}(w)$  in  $w$ , measured in [20], generalizes Kolmogorov's law, hence our terminology.  
[29] P. Le Doussal and K. J. Wiese, Phys. Rev. E **79**, 051106 (2009).  
[30] Equals the number of rooted planar trees with  $n+1$  bonds and arbitrary coordination, the Catalan numbers.